Cell Transplantation
2018, Vol. 27(9) 1352–1367

DOI: 10.1177/0963689718780304
journals.sagepub.com/home/cll
SAGE

Preconditioning Enhances the Therapeutic Effects of Mesenchymal Stem Cells on Colitis Through PGE2-Mediated T-Cell Modulation

Fu Yuan Yang[1], Rui Chen[1], Xiaohu Zhang[2,3], Biao Huang[1], Lai Ling Tsang[1], Xican Li[4,5], and Xiaohua Jiang[1,6,7]

Abstract

Mesenchymal stem cell (MSC)-based cell therapy has been demonstrated as a promising strategy in the treatment of inflammatory bowel disease (IBD), which is considered an immune disease. While the exact mechanisms underlying the therapeutic effect of MSCs are still unclear, MSCs display anti-inflammatory and immunomodulatory effects by interacting with various immunoregulatory cells. Our previous studies have shown that MSCs can be preconditioned and deconditioned with enhanced cell survival, differentiation and migration. In this study, we evaluated the effect of preconditioning on the immunoregulatory function of human umbilical cord-derived MSCs (hUCMSCs) and their therapeutic effect on treating IBD. Our results show that intraperitoneal administration of deconditioned hUCMSCs (De-hUCMSCs) reduces the disease activity index (DAI), histological colitis score and destruction of the epithelial barrier, and increases the body weight recovery more intensively than that of un-manipulated hUCMSCs. In addition, De-hUCMSCs but not hUCMSCs elicit anti-apoptotic effects via induction of the ERK pathway during the early stage of IBD development. In vitro co-culture studies indicate that De-hUCMSCs suppress T-cell proliferation and activation more markedly than hUCMSCs. Moreover, De-hUCMSCs block the induction of inflammatory cytokines such as tumor necrosis factor (TNF)α and interleukin (IL)-2, while promoting the secretion of the anti-inflammatory cytokine IL-10 in T-cells. Mechanically, we find that prostaglandin E2 (PGE2) secretion is significantly increased in De-hUCMSCs, the suppression of which dramatically abrogates the inhibitory effect of De-hUCMSCs on T-cell activation, implying that the crosstalk between De-hUCMSCs and T-cells is mediated by PGE2. Together, we have demonstrated that preconditioning enhances the immunosuppressive and therapeutic effects of hUCMSCs on treating IBD via increased secretion of PGE2.

Keywords

Preconditioning, MSCs, immune, IBD, PGE2

[1] Key Laboratory for Regenerative Medicine of the Ministry of Education of China, School of Biomedical Sciences, Faculty of Medicine, The Chinese University of Hong Kong, Hong Kong SAR, China
[2] Sichuan University, The Chinese University of Hong Kong Joint Laboratory for Reproductive Medicine, West China Second University Hospital, Sichuan University, Chengdu, Sichuan, China
[3] Key Laboratory of Birth Defects and Related Diseases of Women and Children (Sichuan University), Ministry of Education, West China Second University Hospital, Sichuan University, Chengdu, Sichuan, China
[4] School of Chinese Herbal Medicine, Guangzhou Higher Education Mega Center, Guangzhou, China
[5] Innovative Research and Development Laboratory of TCM, Guangzhou Higher Education Mega Center, Guangzhou, China
[6] Chinese University of Hong Kong, University of Southampton Joint Laboratory for Regenerative Medicine, School of Biomedical Sciences, Chinese University of Hong Kong, Hong Kong SAR, China
[7] School of Biomedical Sciences Core Laboratory, Shenzhen Research Institute, The Chinese University of Hong Kong, Shenzhen, China

Submitted: December 14, 2017. Revised: April 30, 2018. Accepted: May 8, 2018.

Corresponding Author:
Xiaohua Jiang, Room 409A, 4/F, Lo Kwee-Seong Integrated Biomedical Sciences Building, The Chinese University of Hong Kong, ShaTin, N.T. Hong Kong, China.
Email: xjiang@cuhk.edu.hk

Introduction

Inflammatory bowel disease (IBD) is a group of diseases featured by a chronic, relapsing or remitting course of gastrointestinal (GI) symptoms such as diarrhea, rectal bleeding and abdominal cramping[1]. According to the clinical manifestations and pathological traits, IBD is classified as ulcerative colitis (UC) and Crohn's disease (CD). Histologically, UC is mainly restricted in the mucosal layer of colon in a continuous fashion, whereas CD is more featured by discontinuous and ulcerous trans-mural inflammatory lesions. While the etiology and pathogenic mechanisms underlying IBD remain largely elusive, the development of IBD results from an extremely complex interaction among genetics, environments, microbial factors and autoimmune responses, eventually leading to chronic inflammation and tissue destruction in the gastrointestinal tract[2]. Despite enormous efforts in optimizing the existing drugs and developing new drugs in recent years, a large portion of IBD patients are still not responsive to medical treatment. This is largely due to the fact that the current therapeutic drugs, such as corticosteroids, nonsteroidal anti-inflammatory drug (NSAIDs) and anti-tumor necrosis factor (TNF) agents, have a very selective action and routinely aim for one therapeutic objective. Consequently, stem cell therapy has been emerging as a new paradigm for IBD treatment, largely owing to their multifaceted biological functions.

Compared with other sources of stem cells, mesenchymal stem cells (MSCs) exhibit many favorable characteristics including easy accessibility, no ethical issues and immunological compatibility[3]. Of importance, MSC transplantation is considered safe and has been widely tested in clinical trials of cardiovascular, neurological, and immunological diseases with encouraging results[4]. Indeed, MSC-based therapy has been appearing as a novel approach targeting the multiple pathological processes involved in IBD, which aims to replace damaged tissues, inhibit inflammation and suppress fibrosis[5,6]. In 2005, García-Olmo et al. reported the first phase I clinical trial on eight complex fistulas in five CD patients by using adipose tissue-derived MSCs (AT-MSCs) with positive results[7]. From then on, numerous studies have been initiated to investigate the therapeutic effects and biological functions of MSCs derived from diverse sources including bone marrow, adipose tissue, umbilical cord, gingiva and human embryonic stem cells[5,8–10]. In colitis models, MSCs have been observed to differentiate into cells that can repair intestinal damage and restore the integrity of the epithelial barrier[11]. Moreover, MSCs display anti-inflammatory and immunomodulatory effects, especially immunosuppressive properties by interacting with various immunoregulatory cells. In particular, MSCs produce a wide range of factors that have been implicated in immunomodulating effects, such as indoleamine 2,3-dioxygenase[12], interleukin (IL)-10[13], prostaglandin E2 (PGE2)[14,15] transforming growth factor (TGF)-β_1[16] and nitric oxide.[17] Among them, PGE2 has been shown to modulate immune response via its action on various immune cells. For instance, PGE2 not only plays an active role in the maturation of dendritic cells, but also up-regulates the production of immunosuppressive IL-10 in dendritic cells[18]. In addition, PGE2 inhibits IL-2 production and T-helper cell proliferation, whereas promotes the production of regulatory T-cells[15,19].

MSC therapy for IBD represents a promising strategy. However, for the ultimate application of MSCs in a clinical setting, there are still many hurdles for us to overcome. For instance, despite enormous potential, many animal studies reported low levels of MSC recruitment and persistence in vivo[20]. Therefore, methods for enhancing the survival and anti-inflammatory effects of MSCs are urgently needed to improve their clinical efficacy. Previous studies from both our group and others demonstrated that priming MSCs with defined preconditioning media improved cell survival, migration, differentiation capacities and secretory function of MSCs[21–25]. Given that the therapeutic effects of MSCs on IBD are largely associated with their secretory function which contributes to immune and inflammation modulation, we reasoned that the preconditioning strategy might impact on the therapeutic effects of MSCs on IBD treatment. Thus, we undertook the present study to evaluate the effect of preconditioning on the immunoregulatory function of MSCs and their therapeutic efficacy in treating IBD.

Materials and Methods

Cell Culture

Human umbilical cord mesenchymal stem cells (hUCMSCs) were purchased from ATCC (PCS-500-010, Manassas, VA, USA). Cells were cultured at 37°C, 5% CO_2 in minimal essential medium alpha, with 10% fetal bovine serum (FBS) and 1% penicillin-streptomycin. Cells were passaged every 2–3 days when they reached 70–80% confluence. Passages between 5 to 12 were used in this study. Jurkat and HCT116 (purchased from Institute of Biochemistry and Cell Biology, CAS, Shanghai, China) cells were cultured with RPMI-1640, 10% FBS and 1% penicillin-streptomycin. Cells were passaged when they reached 70–80% confluence.

Preconditioning and Deconditioning

The hUCMSCs were seeded at 6×10^5 cells per 75 cm^2 flask and b-fibroblast growth factor (FGF) (10 ng/ml) (PeproTech, Rocky Hill, NJ, USA) and all-trans-retinoic acid (ATRA, 10^{-7} M) (Sigma, St. Louis, MO, USA) were added to culture medium 24 hours later. After another 24 hours, cells were rinsed with phosphate-buffered saline (PBS) and cultured with modified neuronal medium (MNM) for preconditioning (primed-hUCMSCs) for another 24 hours[23]. The MNM was then washed out and replaced with α-minimum essential medium (MEM), cells were allowed to grow for another 2 days (deconditioning phase) and indicated as deconditioned MSCs (De-hUCMSCs). For re-preconditioning, the De-hUCMSCs were cultured in MNM for another 24 hours. To collect conditional medium, hUCMSCs or De-hUCMSCs

were washed with PBS three times, and 10 ml serum-free α-MEM per 1.5×10^6 cells was added. The medium was collected 24 hours later, and filtered as conditional medium.

MTT

MTT assay (Sigma-Aldrich, St. Louis, MO, USA) was used to evaluate cell viability. Cells were seeded in 96-well plates at a density of 5000 cells per well. Cells were rinsed with PBS 24 h post seeding and 100 µl conditional medium was added. After culture for the indicated period, MTT was added to and the optical density (OD) value was detected at 570 nm as suggested by the vendor.

Jurkat and hUCMSCs/De-hUCMSCs Co-culture

The 5×10^6 Jurkat cells were seeded in 1640 medium with 10% FBS and 1% P/S, 25 µg/ml Phorbol 12-myristate 13-acetate (PMA) and 1 µM ionomycin were applied to activate Jurkat for 24 hours. The 4×10^5 hUCMSCs or De-hUCMSCs per well were seeded in six-well plates. After 24 h, hUCMSCs/De-hUCMSCs were washed with PBS twice. Activated Jurkat cells were directly seeded on hUCMSCs/De-hUCMSCs (1×10^6 per well). After 48 h, Jurkat cells were transferred to a 96-well plate (100 µl per well), 25 µl (3-[4,5-dimethylthiazol-2-yl]-5-[3-carboxymethoxyphenyl]-2-[4-sulfophenyl]-2H-tetrazolium, inner salt [MTS]) was then added, and OD values were read at 490 nm.

HCT116 Treated with Conditional Media

The 5×10^5 HCT116 cultured in Roswell Park Memorial Institute (RPMI)-1640 medium was washed with PBS and cultured in serum-deprived media with 100 µg/ml TNF-α for 24 hours. Conditional media from hUCMSCs or De-hUCMSCs was then added into treated HCT-116 for 24 h. Cell proliferation was measured by MTT assay.

Flow Cytometry

Cells were collected and washed with PBS, then re-suspended in the staining buffer (PBS with 1% bovine serum albumin; BSA) at a concentration of 5×10^5 cells/100 µl. Fluorescein-conjugated antibodies were added to the cell suspension and incubated at room temperature for 30 min in the dark. Cells were washed with PBS once, re-suspended in 400 µl of staining buffer and analyzed by flow cytometry. Annexin V-APC/PI Kit was used to evaluate cell apoptosis. Experiments were carried out following the manufacturer's instructions. Fluorescent signals were detected with a flow cytometer (LSR Fortessa Cell Analyzer, BD, CA, USA).

Semi-Quantitative Polymerase Chain Reaction (PCR) and Quantitative Real-Time (qRT) PCR

Total RNA was isolated using TRIZOL Reagent (Invitrogen, Waltham, MA, USA), 1–5 µg total RNA were used for reverse transcription, first-strand complementary DNA synthesis was performed using oligd$(T)_{18}$ and M-MLV enzyme (Promega, Madison, WI, USA). A PRISM PCR system was applied to amplify target genes (thermal cycling program: 1: 94°C 4 min; 2: 94°C 30 s; 3: 55°C 30 s; 5: 72°C 30 s; 4: 72°C 10 min; 2–5 was repeated 30–35 cycles). PCR products were separated by agarose gel electrophoresis and analyzed by detection system software version 2.2.1 (Applied Biosystems, Foster City, CA, USA). For qRT-PCR, the levels of mRNA were measured by real-time PCR (Applied Biosystems) using SYBR Green Master Mix (Applied Biosystems). The total amount of mRNA was normalized to endogenous glyceraldehyde 3-phosphate dehydrogenase mRNA. The sequences of the primers were shown in Supplementary Table 1.

PCR Array

Total RNA was isolated using the RNeasy mini kit according to manufacturer's instructions (Life Technologies, Carlsbad, CA, USA). The quantity of RNA was determined by spectrophotometer at 260 nm and the OD 260/280 ratio was measured to determine RNA quality. Then 1 µg total RNA of each sample was transcribed into cDNA using RT^2 First Strand Kit (Qiagen, Hilden, Germany). Real-time PCR array analysis was performed according to the manufacturer's protocol with the RT^2 Real-Time SYBR green PCR Master Mix on Applied Biosystems' 7500 Fast Real-Time PCR System. Expression of 84 genes was analyzed using the MSC (PAHS-082C) RT^2 profiler PCR array. Data were normalized using multiple housekeeping genes and analyzed by comparing $2^{-\Delta Ct}$ of the normalized data. Fold changes were calculated relative to the untreated MSCs. An arbitrary cut-off of >1.8-fold change was used to identify genes that were differentially expressed between samples.

Western Blot

Cells or tissues were lysed at 4°C using radioimmunoprecipitation assay lysis RIPA (Thermofisher, Waltham, MA, USA) buffer with a protease inhibitor cocktail for 30 min. Supernatants were collected and the concentrations of protein were measured by Bradford protein assay system (Bio-Rad, Hercules, CA, USA). Proteins were incubated with primary antibodies overnight at 4°C, then washed and incubated with horseradish peroxidase-conjugated secondary antibodies diluted 1:10,000 in 2% milk tris-buffered saline tween-20. Antibodies used in the western blot are listed in Supplementary Table 2. The membranes were washed, protein bands were detected by enhanced chemiluminescence reagent (Amersham, Little Chalfont, UK) and SuperRX-film (Fuji Medical, Stamford, CT, USA). For quantification, densitometry in ImageJ was applied to quantify the relative intensities of bands.

Enzyme-Linked Immunosorbent Assay

2×10^5 hUCMSCs or 1.5×10^5 De-hUCMSCs were seeded in one well of the six-well plates. After 24 hours, cells were rinsed with PBS and 1 ml serum-free α-MEM medium (Thermofisher, Waltham, MA, USA) was added. Medium was collected 48 h later and used immediately or stored at −80°C. Colons were homogenized in PBS with 0.5% 100x Triton (Sigma, St. Louis, MO, USA) and protease inhibitor cocktail. Lysates were incubated at 4°C for 30 mins, followed by 14,000 rpm centrifuge at 4°C. Supernatant was collected and protein concentration was measured by the Bradford protein assay system (Bio-Rad). The enzyme-linked immunosorbent assay (ELISA) kits used were Mouse IL-6, IL-10 ELISA Kits (ThermoFisher Scientific, Waltham, MA, USA; EM2IL6, EM2IL10, EMTNFA), Mouse IL-17a ELISA kit (Invitrogen, Carlsbad, CA, USA; KMC3021), Prostaglandin E_2 EIA Kit-Monoclonal (Cayman, Ann Arbor, MI, USA; 514010) and Human IL-2, IL-10 (ThermoFisher Scientific; EH2IL2, EHIL10).

Dextran Sulfate Sodium-induced IBD Mouse Model

Mature female C57 mice (weight 19–21 g, purchased from Laboratory Animal Services Center of the Chinese University of Hong Kong) were used in this study. All animal experiments were conducted in accordance with the guidelines and regulations on animal experimentation of the Chinese University of Hong Kong and approved by the Animal Ethnics Committee of the University (15-225-MIS). Mice were fed with 1.5% dextran sulfate sodium (DSS) (w/v) in drinking water (ddH_2O) for 6 consecutive days to establish the model. Weights of the mice were measured every day throughout the whole experiment. Mice were randomly divided into three groups, PBS group; hUCMSCs group; and De-hUCMSCs group. On the 2nd and 6th day of DSS feeding, 100 µl of PBS or 2×10^6 hUCMSCs or De-hUCMSCs in 100 µl PBS were intraperitoneally (IP) injected into each mouse. At different time points, mice were sacrificed with CO_2, and colons and spleens were collected for further studies.

Primary Culture of Splenocytes

C57 mice were fed with 1.5% DSS in drinking water for 6 consecutive days to activate the inflammatory response. Mice were sacrificed and spleens were collected. A syringe with a 24G needle was applied to insert PBS into the spleens, and washed till spleens turned white. The solution was collected and centrifuged at 500 *g* at room temperature for 5 min. Red blood cells were lysed with ammonium chloride (0.75%, w/v), and left cells were rinsed by PBS three times and re-suspended in RPMI 1640 with 10% FBS. After collection, splenocytes were seeded on either hUCMSCs or De-hUCMSCs at the ratio of 4:1.

Disease Activity Index

The disease activity index (DAI) of IBD was assessed according to a previously established method[26]. Briefly, DAI is the summation of three parameters (0–4 score for each): body weight loss, stool consistency and occult bleeding. Weight loss score (0: <5%; 1: 5–10%; 2: 10–15%; 3: 15–20%; 4: >20%), stool consistency score (0: normal; 2: loose; 4: diarrhea), occult bleeding was detected by a Hemoccult II SENSA kit (Beckman, Brea, CA, USA) and scored according to the blue color intensity.

Histology Score

Histological analysis of IBD severity was based on the following parameters as described in a previously study[27]: (1) epithelial damage (0: none; 1: minimal loss of goblet cells; 2: massive loss of goblet cells; 3: slight loss of crypts; and 4: massive loss of crypts), and (2) infiltration (0: none; 1: crypt base infiltration; 2: mucosa infiltration; 3: severe mucosa infiltration and edema; and 4: submucosa infiltration).

Hematoxylin and Eosin (H&E) Staining

Paraffin-embedded colons were prepared in 6-µm sections, de-paraffinized using xylene and rehydrated through gradient alcohol (100% × 2, 95% × 2, 80% × 1, 70% × 1, water × 1, 90 s per step with shaking). The frozen sections (6 µm) were firstly washed with PBS for 5 min, then dipped into water for 2 min. After rehydration, sections were stained with hematoxylin for 5 min, and differentiated in acid ethanol for 3 min. Then the sections were washed in running tap water for 2 min, blued in tap water for 10 min and stained in eosin Y solution for 1–2 min. 95% × 2 plus 100% × 2 alcohol was added for dehydration, cleared with xylene twice and finally mounted with histological mounting medium.

Immunofluorescence Staining

Sections were rehydrated as described for H&E staining, then rinsed with PBS twice. Antigen retrieval was carried out by soaking and heating samples to 95°C in antigen-refined buffer (pH 9) and cooled to room temperature. Slides were washed in PBS for three times, blocked with 2% donkey serum in PBS with 0.1% Triton for an hour. Primary antibody incubation was carried out at room temperature for 2 h, or 4°C overnight, then rinsed in PBS three times. A secondary antibody was added to sections and incubated at room temperature for 1 h. Samples were rinsed in PBS three times and mounted with 4',6-diamidino-2-phenylindole (DAPI)-containing mounting medium. Results were collected by fluorescent microscope (Nikon, Tokyo, Japan; 80i) and signals were indicated as a percentage of positive stained cells. Images were evaluated in five different fields, and >100 cells were evaluated for each slide. Primary and secondary antibodies are listed in Supplementary Table 2.

Terminal Deoxynucleotidyl Transferase dUTP Nick End Labeling (TUNEL)

Sections were rehydrated as described for H&E staining. TUNEL staining was carried out using an in-situ cell death detection kit (Roche, Basel, Switzerland), then mounted with DAPI-containing medium.

Statistical Analysis

All experiments were repeated at least three times, data are presented as mean ± SEM. A Student's *t* test was applied to calculate the differences between two groups while a one-way analysis of variance (ANOVA) was applied for comparison among three groups, and post-hoc analyses were performed with Newman–Keuls multiple comparison test. Statistically significant was considered as $P < 0.05$ (*indicates $P < 0.05$, **indicates $P < 0.01$ and ***indicates $P < 0.001$). Statistical calculations were performed with GraphPad Prism software.

Results

Preconditioning Enhances Cell Survival and Alters the Secretory Function of MSCs

In this study, we decided to use hUCMSCs due to the fact that hUCMSCs have many advantages compared with human bone marrow-derived MSCs (hBMSCs)[28]. In particular, hUCMSCs have been extensively evaluated for treating IBD in both preclinical and clinical studies[15,29–31]. To affirm the effect of preconditioning on hUCMSCs, we employed the protocol previously used for BMSCs[22,23]. When hUCMSCs were subjected to all-trans-retinoic acid followed by MNM, they underwent dramatic morphological changes. Withdrawal of MNM rapidly reverted the primed MSCs back to mesenchymal morphology (deconditioned MSCs, De-hUCMSCs) (Fig. 1A). We then compared the cell-surface markers between De-hUCMSCs and their un-manipulated counterparts at passage 1 to 2, and found that there was no difference in CD marker expression between De-hUCMSCs and hUCMSCs (Fig. S1A and B), indicating that the preconditioning procedure does not change hUCMSC phenotype. To further determine whether the De-hUCMSCs are distinctive from the un-manipulated hUCMSCs, we first evaluated their proliferative capacity using MTT assay. Our result showed that while De-hUCMSCs grew faster at day 1, the growth rate slowed down on the following dates compared with hUCMSCs (Fig. 1B). We then determined the apoptotic response of hUCMSCs and De-hUCMSCs when challenged with hydrogen peroxide (H_2O_2). Under the stress of 500 μM H_2O_2, De-hUCMSCs showed much higher resistance to apoptotic stimuli compared with hUCMSCs (Fig. 1C).

To further characterize the molecular identities of De-hUCMSCs, we used a focused real-time PCR array encompassing 84 genes associated with MSC identity (PAHS-082C). As shown in Fig. S3A, 13/84 MSC-related genes (15.5%) were differentially expressed between hUCMSCs and De-hUCMSCs. Among them, various transcripts that are associated with MSC secretion, were globally changed. For instance, the expression levels of *BMP2*, *BMP6*, *TGFB3* were significantly upregulated in De-hUCMSCs, indicting preconditioning alters the secretory function of MSCs (Fig. S2A and B). In addition, we also compared the expression levels of various genes involved in cellular stress response and inflammation regulation. Interestingly, several cytokines involved in inflammation modulation were differentially expressed between hUCMSCs and De-hUCMSCs (Fig. S2B). Taken together, these data suggest that preconditioning enhances cell survival and alters the secretory function of MSCs.

De-hUCMSCs Ameliorate Colitis More Profoundly than hUCMSCs in a DSS-induced IBD Mouse Model

To test the potential therapeutic effect of hUCMSCs/De-hUCMSCs on IBD, we used a DSS-induced mouse model. In this model, with 1.5% (w/v) DSS, mice presented the most evident clinical signs of colitis from day 5 to day 8, along with a significant weight loss that peaked from day 7 to day 10. Thus, we decided to administer hUCMSCs/De-hUCMSCs twice on day 2 and day 6 (Fig. 2A). Our results showed that while hUCMSC-treated mice exhibited a mild reduction in weight loss and faster body weight recovery compared with PBS-treated mice, De-hUCMSCs demonstrated a more pronounced effect on reduction of weight loss and faster weight recovery from day 8 to 12 (Fig. 2B). In order to further monitor the effects of De-hUCMSCs/hUCMSCs on IBD clinical symptoms, the DAI was scored daily with three parameters: weight loss, stool consistency and occult bleeding. In hUCMSC-treated mice, the DAI was only significantly reduced on day 8 and day 12, as compared with PBS-treated mice. However, in De-hUCMSC-treated mice, the DAI was more consistently and markedly decreased during the recovery phase (Fig. 2C).

To further investigate the protective effects of hUCMSCs/De-hUCMSCs on DSS-induced IBD, colon tissues were collected at day 5, 8 and 12 for histopathological examination in different treatment groups (Fig. 2A). We did not find any significant difference in colon length among different treatment groups (Fig. S3A). However, histopathological examination of the colon sections in the distal and proximal tracts showed that the preconditioning significantly reduced the extension and the severity of the inflamed area and the infiltration of inflammatory cells, as compared with PBS or hUCMSC-treated mice (Fig. 2D, E, Fig. 3A and Fig. S3B). H&E staining indicated that De-hUCMSCs effectively reduced epithelial damage while hUCMSCs showed relatively mild protection. On day 8, while most of the crypts were damaged in the PBS-treated group, crypt structures were largely preserved in both hUCMSC and De-hUCMSC-treated colons with protective effects being more pronounced in De-hUCMSC-treated mice (Fig. 2D and Fig.

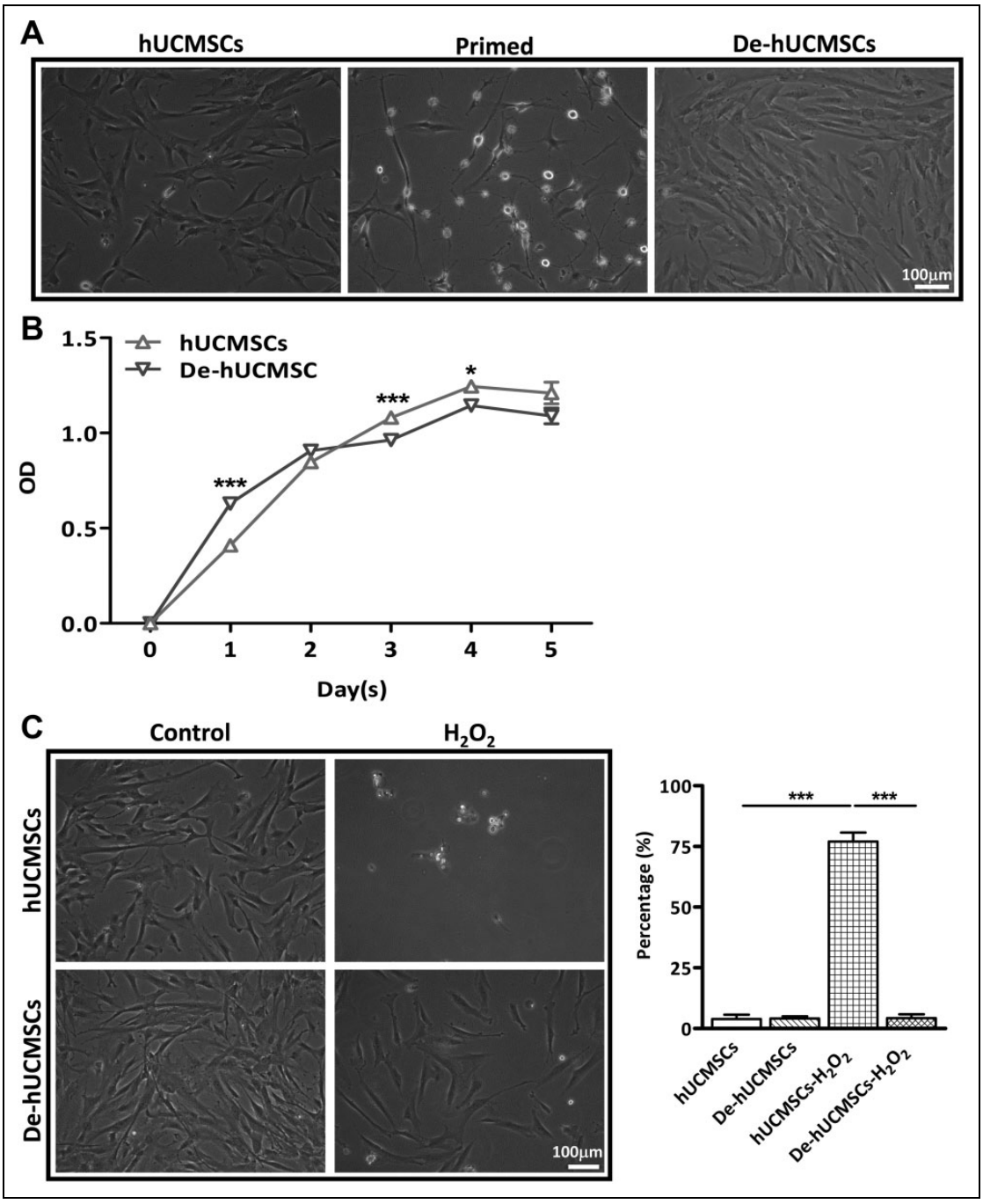

Fig. 1. Preconditioning and deconditioning enhance cell survival of hUCMSCs. hUCMSCs were plated and induced in 75 cm^2 flasks, preconditioning was performed as described in Materials and Methods. (A) Phase contrast photographs of preconditioning and deconditioning of hUCMSCs. Scale bar = 100 μm. (B) Analysis of hUCMSCs or De-hUCMSCs proliferation by MTT assay, experiments were repeated for three times. *$p < 0.05$, ***$p < 0.001$ versus hUCMSCs. (C) Phase contrast photographs of H_2O_2-treated hUCMSCs or De-hUCMSCs. De-hUCMSCs are more resistant to H_2O_2 treatment than hUCMSCs. Scale bar = 100 μm. Quantification data was shown in the right panel. The experimental procedure was repeated three times.
**$p < 0.01$, ***$p < 0.001$; $^{\#\#}p < 0.01$, $^{\#\#\#}p < 0.001$.
De-hUCMSC: deconditioned hUCMSC; hUCMSC: human umbilical cord-derived mesenchymal stem cell.

S3B). A quantitative evaluation of histological damage was performed, and the histological score confirmed that De-hUCMSC treatment significantly reduced the intestinal damage, whereas hUCMSCs did not have this effect (Fig. 2E). In addition, we found that neutrophil infiltration was more remarkably suppressed in De-hUCMSC-treated mice

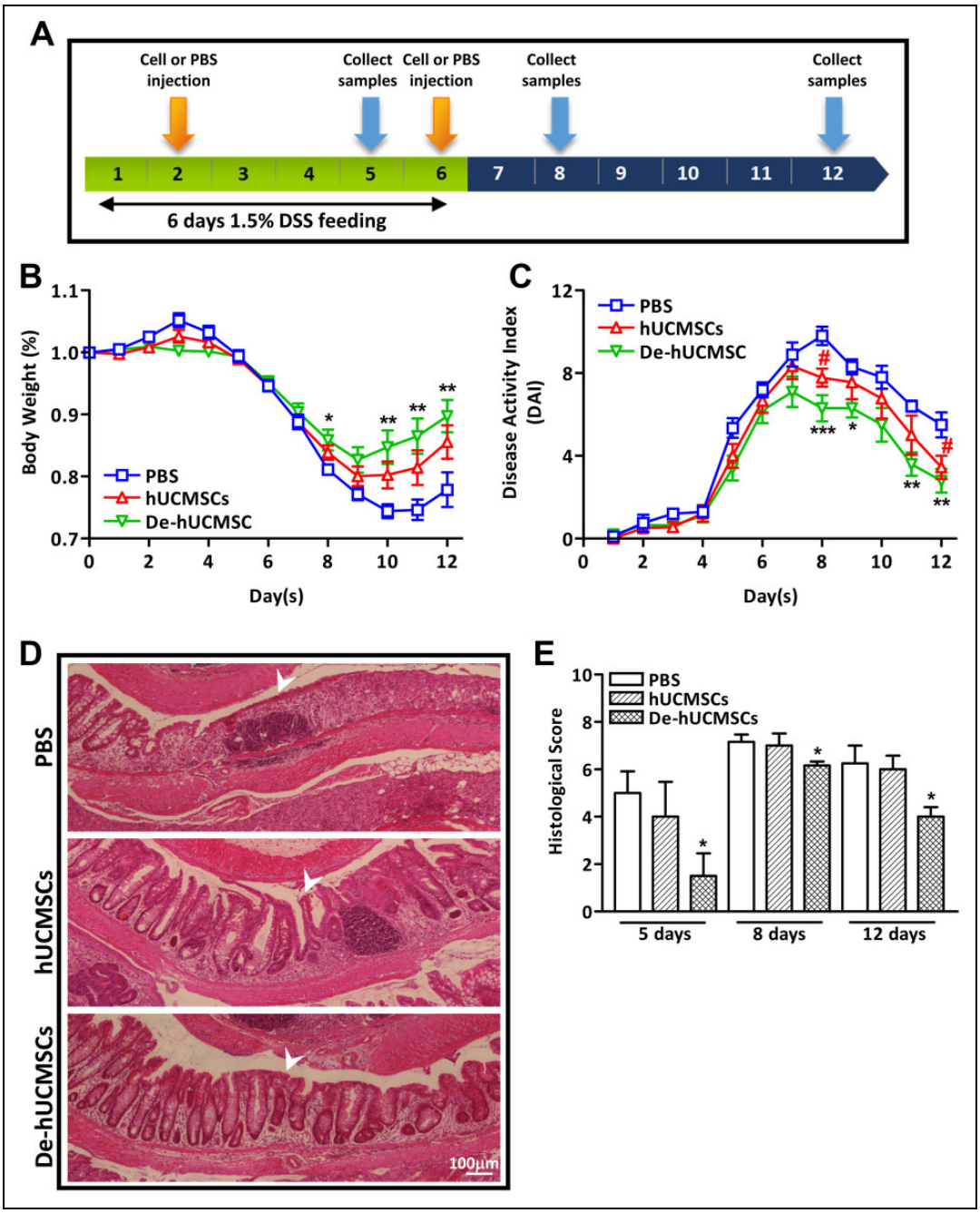

Fig 2. De-hUCMSCs ameliorate colitis more profoundly than hUCMSCs in a DSS-induced IBD mouse model. (A) Schematic of the experiment illustrating the experimental design. (B–C) Mice received 1.5% (w/v) of DSS orally for 6 days. At day 2 and day 6, mice were subjected to 2×10^6 hUCMSCs or De-hUCMSCs or PBS administration. (B) The evolution of colitis is monitored by body weight change relative to the initial body weight at day 0. Data are expressed as mean $\pm$ SEM (IBD, $n = 11$; hUCMSCs, $n = 10$; De-hUCMSCs, $n = 12$). Changes among three groups were analysed by one-way ANOVA followed by the Student Newman–Keuls multiple comparison tests, *represents De-hUCMSCs versus PBS, $p < 0.05$; **represents De-hUCMSCs versus PBS, $p < 0.01$. (C) DAI is calculated by the combined scores of weight loss, stool consistency, and bleeding, as detailed in Material and Methods. Data are expressed as mean $\pm$ SEM, $n = 10$ for each group. Changes among three groups were analysed by one-way ANOVA followed by the Student Newman–Keuls multiple comparison tests. *represents hUCMSCs versus PBS, #represents De-hUCMSCs versus PBS. (D). Photographs of H&E-stained paraffin sections of mouse colons from mice treated with PBS or hUCMSCs/De-hUCMSCs on day 8. Arrows indicate the mucosal destruction and edema in PBS group, whereas the administration of hUCMSCs/De-hUCMSCs inhibits the histological damage. (E) Histology scores are blindly determined from haematoxylin and eosin-stained paraffin sections of mouse intestines harvested on day 5, day 8 and day 12. Histological scores, ranging from 0 (unaffected) to 8 (severe colitis), are derived from the sum of the epithelial damage and infiltration score (day 5 and 12, $n = 4$; day 8, $n = 6$). *$p < 0.05$ versus PBS group.
DAI: disease activity index; De-hUCMSCs: deconditioned hUCMSCs; DSS: dextran sulfate sodium; H&E: hematoxylin and eosin; hUCMSCs: human umbilical cord-derived mesenchymal stem cell; IBD: inflammatory bowel disease; PBS: phosphate-buffered saline.

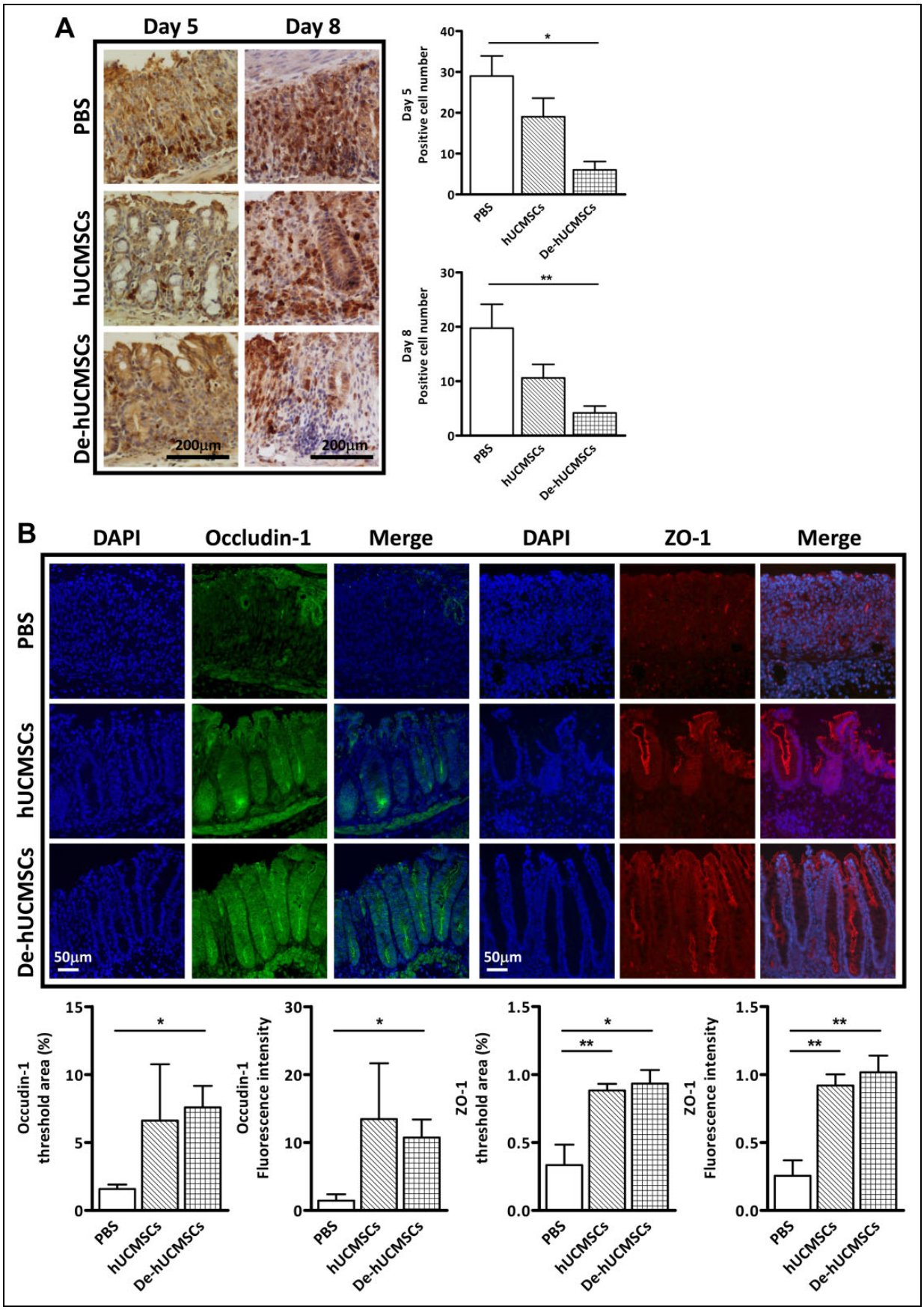

Fig. 3. De-hUCMSCs reduce neutrophil infiltration and protect tight junction integrity. (A) Neutrophils was stained with Ly-6B.2 in paraffin sections of mouse colons harvested on day 5 and day 8. Scale bar = 200 μm. Quantification data are represented at the right panel. A total of

than hUCMSC-treated mice (Fig. 3A). As tight junction proteins play an important role in epithelial barrier function and intestinal homeostasis during IBD onset and development, we evaluated the expression of tight junction proteins Occludin-1 and ZO-1 to assess the integrity of epithelial barrier function. Our results showed that the expression levels of Occludin-1 and ZO-1 were dramatically increased in both hUCMSC and De-hUCMSC-treated colons compared with PBS-treated colons on day 8, which represents the most severe stage of intestinal injury in the DSS model. However, the effect of De-hUCMSCs was more significant (Fig. 3B and Fig. S3C). Altogether, both hUCMSCs and De-hUCMSCs alleviate the DSS-induced colitis, whereas De-hUCMSCs are more effective.

De-hUCMSCs Suppress the Apoptotic Response and Activate the ERK Pathway in the Colon

Having established that De-hUCMSCs elicited better protective effects in DSS-induced colitis, we proceeded to determine the underlying cellular and molecular mechanisms involved in the protective function of De-hUCMSCs. During IBD progression, epithelial cell damage is largely induced by TNF-α-mediated apoptosis, which is closely associated with disease progression and severity. Thus, we determined the apoptotic response by TUNEL staining in control or hUCMSCs/De-hUCMSCs-treated colons. As shown in Fig. 4A, a large number of apoptotic cells were present in the IBD colon on day 5 and day 8. Significantly, while hUCMSCs had no effect on reducing the number of apoptotic cells, De-hUCMSCs dramatically suppressed apoptotic response upon DSS treatment on day 5, indicating De-hUCMSCs probably activated the anti-apoptotic pathway. To further elucidate the molecular mechanisms underlying the anti-apoptotic effect of De-hUCMSCs, a western blot was performed using colon samples collected on day 5, day 8 and day 12, which represented the different stages of the inflammatory process. In consistence with the TUNEL staining, the expression levels of cleaved caspase-3 and p21 were significantly reduced in De-hUCMSC-treated colons but not hUCMSC-treated colons on day 5 and day8 (Fig. 4B), confirming that De-hUCMSC treatment suppresses the apoptotic response. Interestingly, our western blot result revealed that the expression of p-ERK was significantly increased in De-hUCMSC-treated mice compared with PBS-treated mice, whereas hUCMSC treatment did not have this effect (Fig. 5A). We did not find any significant change in p65 or the c-Jun N-terminal kinase (JNK) pathway, which are both implicated in the regulation of the apoptotic response in the intestine (Fig. 5A and Fig. S4A). Since activation of the ERK pathway plays a critical role in the survival of intestinal epithelial cells[32,33], it is plausible that the pro-survival effect of De-hUCMSCs is mediated by the ERK pathway. However, it should be noted that the activation of p-ERK could only be detected on day 5, but not on day 8 and day 12 (Fig. S4A), indicating that the anti-apoptotic effect of De-hUCMSCs was mainly executed in the early stages of IBD.

De-hUCMSCs Suppress Early Immune Response During Colitis Progression

In order to understand the role of hUCMSCs/De-hUCMSCs in intestinal epithelial protection, we first determined the paracrine effect of stem cells on intestinal epithelial cells using HCT116. We mimicked an inflammatory environment by treating HCT116 with TNF-α and evaluated whether hUCMSCs/De-hUCMSCs would protect HCT116 from TNF-α-induced apoptosis. Our MTT assay results showed that while hUCMSCs did not have any effect, De-hUCMSCs promoted HCT116 cell survival slightly in response to TNF-α treatment (Fig. 5B). However, neither hUCMSCs nor De-hUCMSCs had any effect on TNFα-induced apoptosis in HCT116 cells (Fig. 5C). These results suggest that hUCMSCs/De-hUCMSCs might not directly affect epithelial cell survival. During colitis, ulcerated lesions are accompanied by a prominent infiltration of inflammatory cells, including T-lymphocytes, macrophages, and neutrophils. Furthermore, mechanisms underlying recruiting and activating inflammatory cells are believed to involve a complex interplay of inflammatory mediators such as chemokines and cytokines. One component of the immune infiltration is $CD3^+$ T-lymphocytes which are critical effectors of the mucosal immune activation. Our western blot analysis in DSS-induced colon samples showed that both hUCMSC and De-hUCMSC treatment significantly decreased the expression of CD3 on day 5 (Fig. 5D), while this effect was more pronounced in De-hUCMSC-treated IBD colons. However, this effect diminished at the recovery stage of inflammation (data not shown), indicating hUCMSCs/De-hUCMSCs suppresses early but not late immune response.

De-hUCMSCs Modulate T-cell-Mediated Immune Response Through PGE2 Secretion

As HCT116 co-culture experiments indicate that the protective effect of De-hUCMSCs on DSS-treated colitis is not likely attributable to the direct interaction between stem cells and epithelial cells, we further explored the involvement of

Fig. 3. (Continued). five fields per slide were randomly selected and counted, *$p < 0.05$ versus PBS; **$p < 0.01$ versus PBS. (B) Fluorescent microscopy images of Occludin-1 staining (green) and ZO-1 staining (red) in paraffin sections of mouse colons from mice. Nuclei are counter stained with DAPI. Scale bars = 50 μm. Quantification data are shown in the lower panel. *$p < 0.05$ versus PBS; **$p < 0.01$ versus PBS. DAPI: 4',6-diamidino-2-phenylindole; PBS: phosphate-buffered saline.

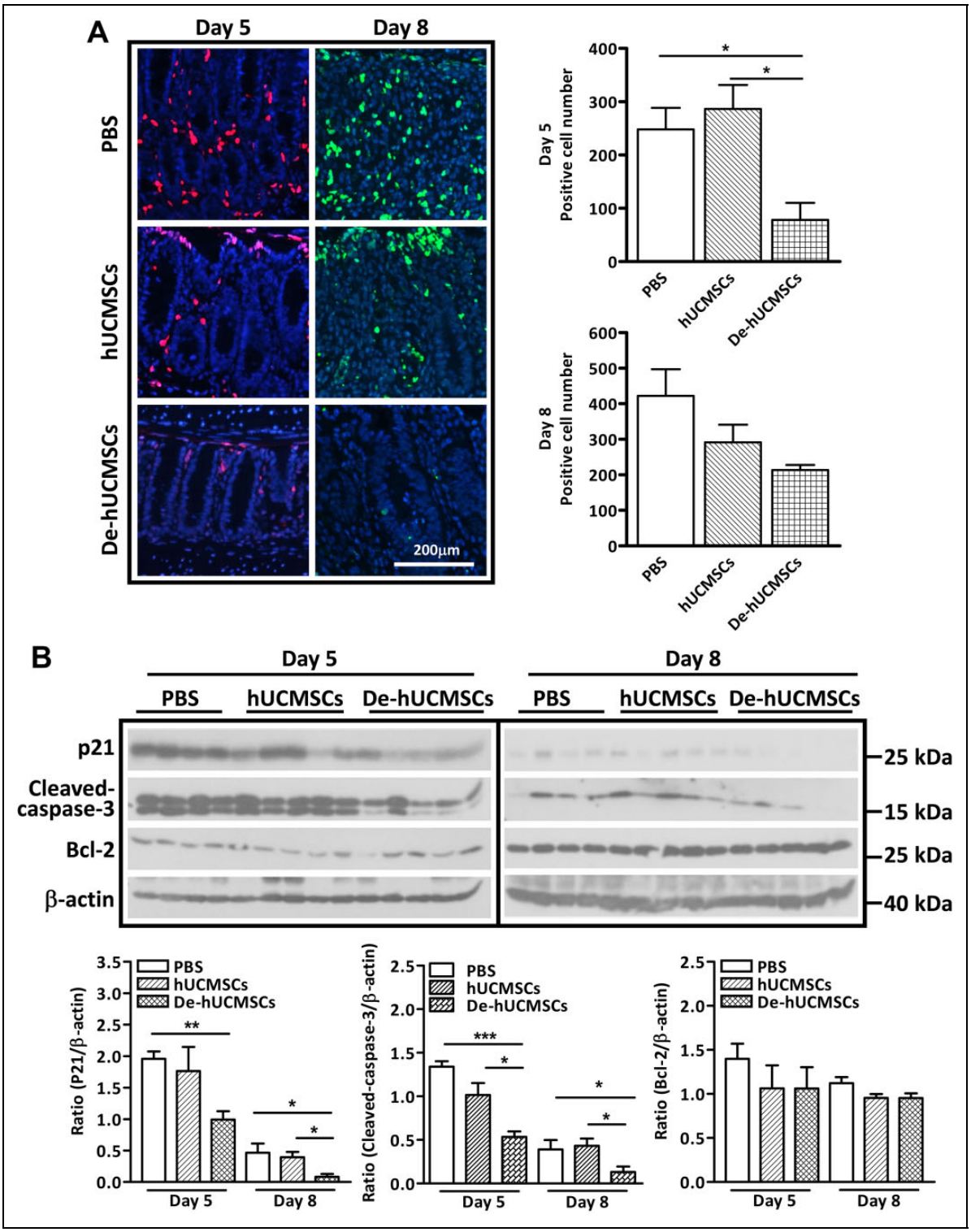

Fig. 4. De-hUCMSCs reduce apoptotic response in DSS-induced colitis colon. (A) Fluorescent microscopy images of TUNEL stained apoptotic cells (red/green) in paraffin sections of mouse colons harvested on day 5 and day 8. Nuclei are counter stained with DAPI. TUNEL positive cells were red on day 5 and green on day 8. Quantification data is shown at the right panel. Five fields per slide were randomly selected and counted, *$p < 0.05$ versus PBS, $n = 3$. (B) Western blot analysis was conducted using whole tissue lysates from DSS-induced colitis mice colon on day 5 and day 8. PBS group: $n = 4$, hUCMSC group: $n = 5$, De-hUCMSC group: $n = 5$. Bar charts represent target protein expression normalized against β-actin. *$p < 0.05$ versus PBS; **$p < 0.01$ versus PBS; ***$p < 0.001$ versus PBS.
DAPI: 4',6-diamidino-2-phenylindole; De-hUCMSCs: deconditioned hUCMSCs; DSS: dextran sulfate sodium; hUCMSCs: human umbilical cord-derived mesenchymal stem cell; TUNEL: Transferase dUTP Nick End Labeling.

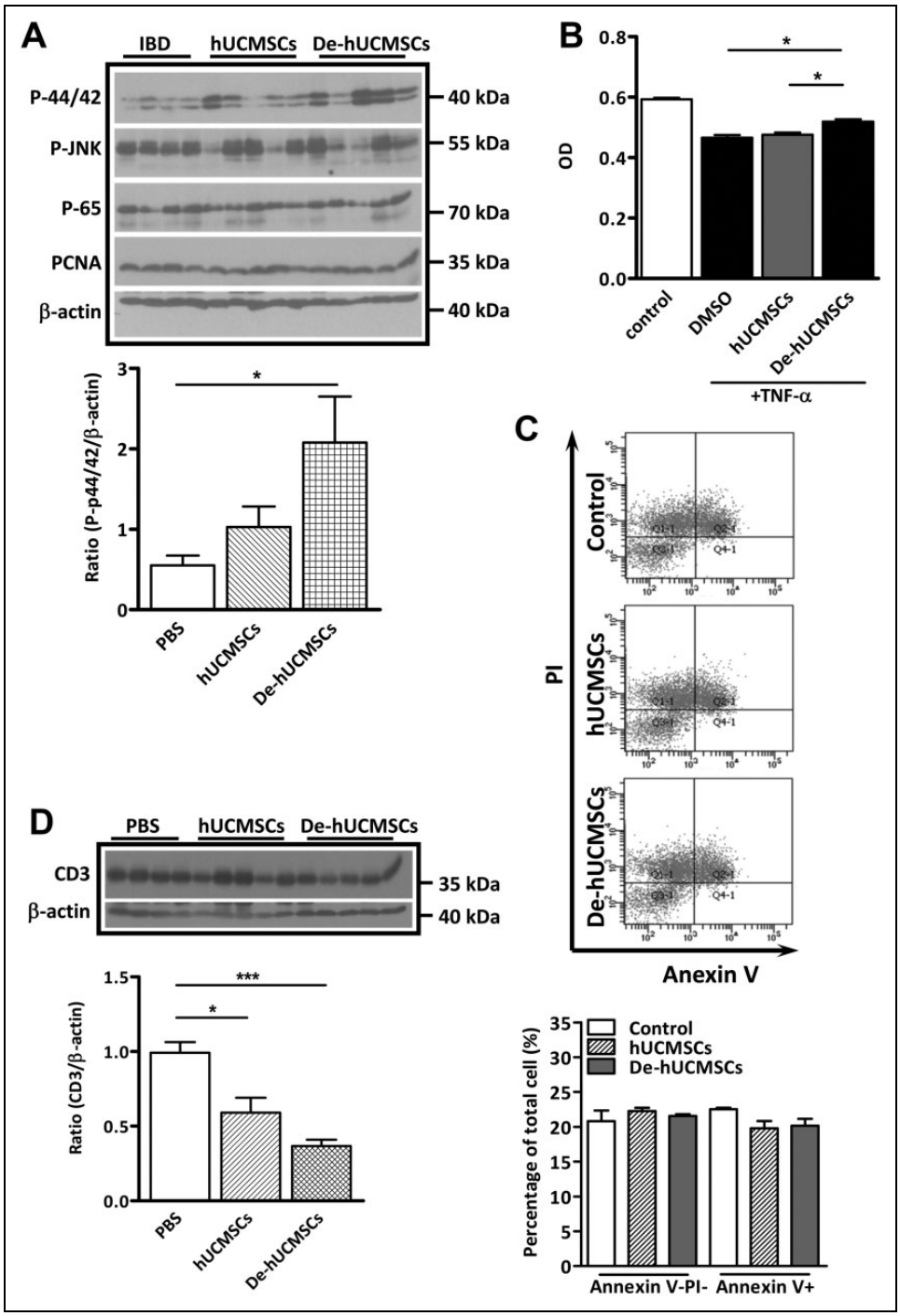

Fig. 5. De-hUCMSCs induce ERK pathway and suppress T-cells. (A) Western blot analysis was conducted using whole tissue lysates from DSS-induced colitis mouse colon treated with PBS/ hUCMSCs/ De-hUCMSCs. PBS group: $n = 4$, hUCMSCs group: $n = 5$, De-hUCMSCs group: $n = 5$. Bar charts represent p-p44/p42 expression normalized against β-actin. *$p < 0.05$ versus PBS. (B) Conditional media from hUCMSCs or De-hUCMSCs was added into 100μg/ml TNF-α-treated HCT116 for 24 h, cell proliferation was measured by MTS assay. *$p < 0.05$, **$p < 0.01$ versus DMSO. (C) Flow cytometry analysis of apoptosis in TNF-α treated HCT116 cells with or without hUCMSCs/ De-hUCMSCs conditional medium. Neither hUCMSCs nor De-hUCMSCs have effects on TNF-α-induced apoptosis in HCT116 cells. (D) Western blot shows the expression of CD3 is significantly decreased in hUCMSCs/De-hUCMSCs-treated mouse colon on day 5. PBS group: $n = 4$, hUCMSCs group: $n = 5$, De-hUCMSCs group: $n = 5$. Bar charts represent CD3 expression normalized against β-actin. *$p < 0.05$, ***$p < 0.001$ versus PBS.

De-hUCMSCs: deconditioned hUCMSCs; DMSO: dimethyl sulfoxide; hUCMSCs: human umbilical cord-derived mesenchymal stem cell; IBD: inflammatory bowel disease; PBS: phosphate-buffered saline; TNF: tumor necrosis factor.

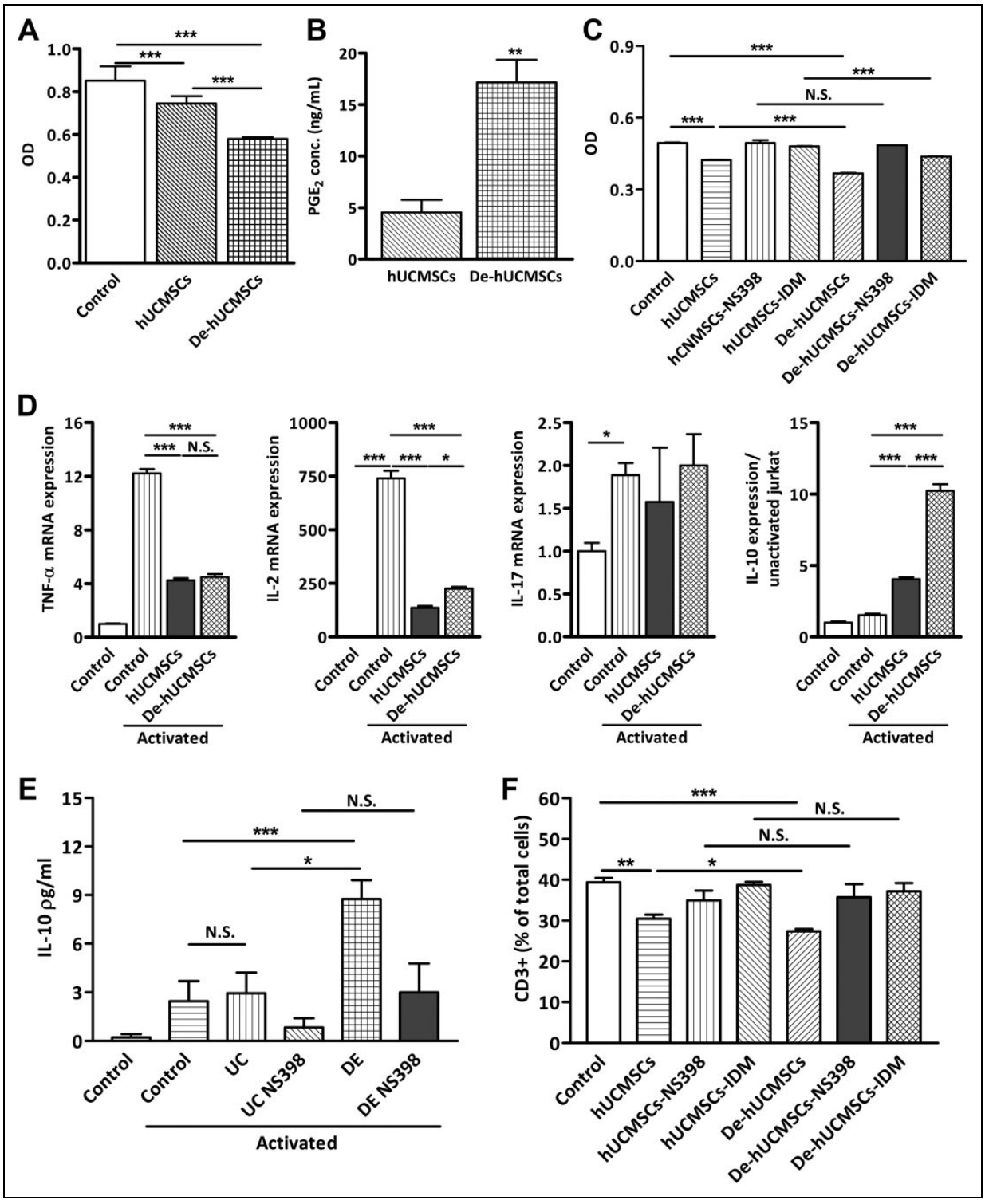

Fig. 6. De-hUCMSCs inhibit T-cell viability and activation through PGE2 secretion. (A) Activated Jurkat cells were cultured in the conditional media derived from either hUCMSCs or De-hUCMSCs for 24 h. An MTS assay was used to determine the total cell number of Jurkat cells. (B) The secretion of PGE2 in conditional medium was determined by an ELISA test in hUCMSCs and De-hUCMSCs. ** $p < 0.05$ versus hUCMSCs. (C) Activated Jurkat cells were cultured in the conditional media derived from either hUCMSCs or De-hUCMSCs (2.5:1) with or without PGE2 inhibitors indomethacin (IDM 50 μM) or NS-398 (50 μM) for 48 h. An MTT assay was used to determine the total Jurkat cell number with different treatments. (D) Activated Jurkat cells were cultured in the conditional media derived from either hUCMSCs or De-hUCMSCs (2.5:1) for 24 h. Real-time PCR was used to determine the expression levels of cytokines. (E) Jurkat cells ($4\times10^4/cm^2$) were seeded on 80% confluent hUCMSCs or De-hUCMSCs. 24 h later, 25 ng/ml PMA and 1 μM ionomycin were added for

T-lymphocytes based on our finding that De-hUCMSCs suppressed the expression of CD3 during early stage of inflammation. We first co-cultured hUCMSCs/De-hUCMSCs with PMA/ionomycin-activated Jurkat cells and evaluated the effect of stem cells on T-cell proliferation by MTS assay. As shown in Fig. 6A, both hUCMSCs and De-hUCMSCs significantly suppressed Jurkat cell viability, whereas the effect of De-hUCMSCs was stronger. Given that PGE2 is a very important inflammatory regulator involved in the maintenance of immune homeostasis, and MSCs have been demonstrated to suppress immune responses via PGE2 secretion in various immune and inflammatory diseases[34–36], we reasoned that the enhanced therapeutic effect of De-hUCMSCs might be due to increased secretion of PGE2. Indeed, we found that De-hUCMSCs secreted a higher level of PGE2 compared with hUCMSCs (Fig. 6B). Thus, we went further to investigate whether the enhanced suppressive effect of De-hUCMSCs was mediated by increased PGE2 secretion. Strikingly, our results showed that PGE2 inhibitors NS-398 and indomethacin reversed the inhibitory effects of hUCMSCs/De-hUCMSCs on Jurkat proliferation (Fig. 6C). In addition, NS-398 completely reversed the differences between hUCMSCs and De-hUCMSCs in suppressing T-cell activation, indicating this effect was mediated by PGE2 (Fig. 6C). Besides T-cell viability, we also determined whether hUCMSCs/De-hUCMSCs were able to modulate the immunoregulatory function of T-lymphocytes. We showed that both hUCMSCs/De-hUCMSCs dramatically suppressed the mRNA expression of proinflammatory cytokines, such as TNF-α and IL-2, in activated Jurkat cells (Fig. 6D). Since IL-10 is an anti-inflammatory cytokine and immunosuppressive factor, which has been implicated in the immune modulatory function of MSCs in IBD treatment[13,37], we also determined the effect of hUCMSCs/De-hUCMSCs on IL-10 expression. Interestingly, both hUCMSCs and De-hUCMSCs co-incubation significantly increased the mRNA expression of IL-10 in Jurkat, whereas the effect of De-hUCMSCs was more prominent (Fig. 6D). This effect was further confirmed by ELISA analysis showing that De-hUCMSCs dramatically increased the secretion of IL-10 in activated Jurkat. Furthermore, suppression of PGE2 by NS-398 completely reversed the promoting effect of De-hUCMSCs on IL-10 secretion (Fig. 6E), further pinpointing the critical role of PGE2 in mediating the immune modulatory effect of De-hUCMSCs. To confirm the results from Jurkat cells, we isolated mouse splenocytes in IBD mice and co-cultured them with either hUCMSCs or De-hUCMSCs for 24 h. Consistent with the Jurkat data, both hUCMSCs and De-hUCMSCs significantly decreased $CD3^+$ splenocytes, whereas the effect of De-hUCMSCs was stronger. This effect was completely reversed by the pre-treatment with PGE2 inhibitors (Fig. 6F). Collectively, these results clearly indicate that hUCMSCs/De-hUCMSCs suppress T-lymphocyte viability and modulate their immunoregulatory function through secretion of PGE2.

Discussion

The etiologic and pathologic process of human IBD is multifactorial, but a critical part of this disease is the disrupted homeostasis of immune responses[38]. MSCs produce large amount of soluble or membrane-bound factors, which are implicated in the modulation of immune responses through interaction with various immune cells[39]. Promisingly, MSCs have been observed to exert potent immunomodulatory and anti-inflammatory effects in different IBD models[40]. In the present study, we introduce a novel strategy to improve the efficacy of MSC-based cellular therapy for IBD treatment. We show that preconditioning improves the therapeutic efficacy of hUCMSCs via a prostaglandin E_2-mediated immunosuppressive effect in IBD treatment.

DSS-induced colitis is the most commonly used animal model for the study of human IBD. In our study, by oral feeding of 1.5% (w/v) DSS for 6 days, we have successfully established IBD mouse model which recapitulates the early, severe and recovery stage of IBD pathology. Compared with hUCMSCs, De-hUCMSCs appeared to offer evident therapeutic advantages in IBD treatment. Firstly, De-hUCMSCs ameliorated colitis manifestation more significantly than hUCMSCs. De-hUCMSC treatment led to a more prominent reduction in body weight loss and better recovery (Fig. 2B and C). Secondly, De-hUCMSCs transplantation resulted in a more profound improvement in DSS-induced colitis pathology, that is, ulceration, dilation, damage of the crypts and infiltration of inflammatory cells were significantly alleviated in De-hUCMSC-treated mouse colon as indicated by a decreased DAI score (Fig. 2D, 2E, and Fig. 3A). Thirdly, the expression of tight junction proteins, such as ZO-1 and Occludin-1, was better conserved in De-hUCMSC-treated colons (Fig. 3B and Fig. S4C), indicating that De-hUCMSCs are more effective than hUCMSCs in protecting the epithelial barrier function. Collectively, our results demonstrate that in comparison with hUCMSCs, De-hUCMSCs are more effective in reducing clinical and pathological signs of colitis, which are highly relevant in view of the use of MSCs for the treatment of IBD patients.

Fig. 6. (Continued). activation, culture medium was collected 24 h later for ELISA tests. (F) Quantification data showing the percentage of $CD3^+$ cells in mouse splenocytes from IBD mice co-cultured with hUCMSCs or De-hUCMSCs by flow cytometry ($n = 3$). hUCMSCs and De-hUCMSCs significantly reduced the number of $CD3^+$ cells. The suppressive effects of hUCMSCs and De-hUCMSCs on $CD3^+$ could be reversed by the PGE2 inhibitor, indomethacin.

De-hUCMSCs: deconditioned hUCMSCs; ELISA: enzyme-linked immunosorbent assay; hUCMSCs: human umbilical cord-derived mesenchymal stem cell; IBD: inflammatory bowel disease; PCR: polymerase chain reaction; PGE2: prostaglandin E2.

Increased apoptosis of epithelial crypt cells and epithelial barrier cells generally occurs in UC and CD[41,42]. In our study, we found that De-hUCMSCs significantly suppressed apoptosis in IBD colons on day 5 (Fig. 4). The anti-apoptosis function of De-hUCMSCs, to some extent, explains the therapeutic effects displayed by De-hUCMSCs. De-hUCMSCs elicit their protective role by dampening the apoptotic response, which in turn alleviates inflammatory response and epithelial damage. Of note, numerous studies have suggested that the TNF-mediated pathways play key roles in inducing apoptosis in epithelial crypts and barrier[43]. The importance of TNF in disease pathogenesis is underlined by the prominent clinical improvement induced by anti-TNF antibodies[44]. However, whereas it seems likely that neutralization of soluble and membrane-bound TNF might be a key mechanism, the potential of the anti-TNF antibodies to induce lymphocyte/monocyte apoptosis in CD has been considered an additional important mechanism[45]. Moreover, other potential mode of actions includes induction of the anti-inflammatory cytokines IL-10 or TGF-β via retrograde signaling or induction of a certain subset of regulatory T-cells[46]. Thus, it remains unclear whether the effect of anti-TNF on mucosal healing is related to reduced epithelial apoptosis, and whether other cellular components in the injured tissues contribute to the healing effects. In this report, we showed that De-hUCMSCs did not affect epithelial cell survival but rather suppressed T-cell activation directly (Fig. 5D and Fig. 6). Our results are consistent with a scenario in which the proinflammatory cytokines secreted by T-lymphocytes play key roles in inducing programmed cell death in epithelial cells. Thus, it is plausible that the anti-inflammatory and immunomodulatory effect of De-hUCMSCs is mainly attributed to the suppression of T-lymphocyte activation and subsequent immune-mediated apoptosis.

Although the mechanisms by which MSCs regulate the immune response during the pathological processes of IBD are still under intensive investigation, it is well established that MSCs are capable of suppressing proliferation, maturation, and activation of immune cells through secretion of assorted soluble factors[12–17]. One interesting finding from our study is that De-hUCMSCs suppress the proliferation and activation of T-lymphocytes via the paracrine secretion of PGE2. The role of PGE2 in mediating the therapeutic effects of MSCs has been illustrated in IBD mouse models[15]. Using both DSS- and 2,4,6-trinitrobenzenesulfonic acid (TNBS)-induced colitis models, Kim et al., recently showed that PGE2 secretion from hUCMSCs shifted the immune balance from T-helper 1 to T-helper 2 responses, along with an increment in T-regulator cell population. Strikingly, inhibition of PGE2 synthesis almost completely diminished the immunosuppressive and therapeutic effects of MSCs, indicating the pivotal role of PGE2 in MSC function[15]. In our study, we found that the preconditioning strategy remarkably increased the PGE2 secretion in hUCMSCs (Fig. 6B). Suppression of PGE2 secretion in De-hUCMSCs completely abrogated the inhibitory effect of De-hUCMSCs on T-cell proliferation (Fig. 6C and 6F), implying that the crosstalk between De-hUCMSCs and T-cells was mediated by PGE2. Indeed, we demonstrated that co-incubation with hUCMSCs/De-hUCMSCs dramatically decreased the secretion of TNF-α and IL-2 in Jurkat cells (Fig. 6D and Fig. S4B). In addition, De-hUCMSCs but not hUCMSCs markedly induced the secretion of anti-inflammatory cytokine IL-10 in Jurkat cells (Fig. 6E). It should be noted that since our DSS model induces mild colitis with a relative long induction phase and a very short acute phase, both hUCMSC and De-hUCMSC treatment only mildly affect cytokine production in colitis colon and plasma (Fig. S4C). Taken together, we suggest that De-hUCMSCs elicit their enhanced protective role in IBD treatment via suppression of PGE2-mediated T-cell proliferation and activation, which subsequently reduces T-cell-mediated apoptotic response in intestinal epithelium. In view of the fact that PGE2 modulates the immune response via almost all kinds of immune cells, it is plausible that other immune cells are also involved in the enhanced therapeutic effects of De-hUCMSCs.

Collectively, we have demonstrated that hUCMSCs can be manipulated in vitro via preconditioning and deconditioning with enhanced immunosuppressive and therapeutic effects on treating IBD via increased secretion of PGE2. Given the critical role of PGE2 in regulating the immune response, it is conceivable that the preconditioning strategy might exhibit improved therapeutic efficacy in treating other autoimmune diseases, such as rheumatoid arthritis. With easy culture manipulation and a low tendency of tumor formation, the preconditioning strategy provides a feasible approach to enhance therapeutic efficacy for stem cell-based regenerative medicine.

Ethical Approval

All animal experiments were conducted in accordance with the guidelines and regulations on animal experimentation of the Chinese University of Hong Kong and approved by the Animal Ethnics Committee of the University (15-225-MIS).

Statement of Human and Animal Rights

All animal experiments were conducted in accordance with the guidelines and regulations on animal experimentation of the Chinese University of Hong Kong.

Statement of Informed Consent

There are no human subjects in this article and informed consent is not applicable.

Declaration of Conflicting Interests

The authors declared no potential conflicts of interest with respect to the research, authorship, and/or publication of this article.

Funding

The authors disclosed receipt of the following financial support for the research, authorship, and/or publication of this article: This work was supported by Hong Kong UGC/GRF grant (466413,

14119516), Hong Kong Food and Health Bureau (01120056, 03140496) and Guangdong Science and Technology Project (2017A050506043).

Supplemental Material

Supplemental material for this article is available online.

References

1. Corridoni D, Arseneau KO, Cominelli F. Inflammatory bowel disease. Immunol Lett. 2014;161(2):231–235.
2. Baumgart DC, Carding SR. Inflammatory bowel disease: cause and immunobiology. Lancet. 2007;369(9573):1627–16240.
3. Keating A. Mesenchymal stromal cells: new directions. Cell Stem Cell. 2012;10(6):709–716.
4. Sharma RR, Pollock K, Hubel A, McKenna D. Mesenchymal stem or stromal cells: a review of clinical applications and manufacturing practices. Transfusion. 2014;54(5):1418–1437.
5. Martinez-Montiel Mdel P, Gomez-Gomez GJ, Flores AI. Therapy with stem cells in inflammatory bowel disease. World J Gastroenterol. 2014;20(5):1211–1227.
6. Ke C, Biao H, Qianqian L, Yunwei S, Xiaohua J. Mesenchymal stem cell therapy for inflammatory bowel diseases: promise and challenge. Curr Stem Cell Res Ther. 2015;10(6):499–508.
7. García-Olmo D, Garcia-Arranz M, Herreros D, Pascual I, Peiro C, Rodriguez-Montes JA. A phase I clinical trial of the treatment of Crohn's fistula by adipose mesenchymal stem cell transplantation. Dis Colon Rectum. 2005;48(7):1416–1423.
8. van Deen WK, Oikonomopoulos A, Hommes DW. Stem cell therapy in inflammatory bowel disease: which, when and how? Current opinion in gastroenterology. 2013;29(4):384–390.
9. Cho YB, Lee WY, Park KJ, Kim M, Yoo HW, Yu CS. Autologous adipose tissue-derived stem cells for the treatment of Crohn's fistula: a phase I clinical study. Cell Transplant. 2013; 22(2):279–285.
10. Panes J, García-Olmo D, Van Assche G, Colombel JF, Reinisch W, Baumgart DC, Dignass A, Nachury M, Ferrante M, Kazemi-Shirazi L, Grimaud JC, de la Portilla F, Goldin E, Richard MP, Leselbaum A, Danese S, Collaborators ACSG. Expanded allogeneic adipose-derived mesenchymal stem cells (Cx601) for complex perianal fistulas in Crohn's disease: a phase 3 randomised, double-blind controlled trial. Lancet. 2016;388(10051):1281–1290.
11. Yabana T, Arimura Y, Tanaka H, Goto A, Hosokawa M, Nagaishi K, Yamashita K, Yamamoto H, Adachi Y, Sasaki Y, Isobe M, Fujimiya M, Imai K, Shinomura Y. Enhancing epithelial engraftment of rat mesenchymal stem cells restores epithelial barrier integrity. J Pathol. 2009;218(3):350–359.
12. Ryu DB, Lim JY, Lee SE, Park G, Min CK. Induction of Indoleamine 2,3-dioxygenase by Pre-treatment with Poly(I:C) may enhance the efficacy of MSC treatment in DSS-induced colitis. Immune Netw. 2016;16(6):358–365.
13. Sala E, Genua M, Petti L, Anselmo A, Arena V, Cibella J, Zanotti L, D'Alessio S, Scaldaferri F, Luca G, Arato I, Calafiore R, Sgambato A, Rutella S, Locati M, Danese S, Vetrano S. Mesenchymal stem cells reduce colitis in mice via release of tsg6, independently of their localization to the intestine. Gastroenterology. 2015;149(1):163–76 e20.
14. Dave M, Hayashi Y, Gajdos GB, Smyrk TC, Svingen PA, Kvasha SM, Lorincz A, Dong H, Faubion WA Jr., Ordog T. Stem cells for murine interstitial cells of cajal suppress cellular immunity and colitis via prostaglandin E2 secretion. Gastroenterology. 2015;148(5):978–990.
15. Kim HS, Shin TH, Lee BC, Yu KR, Seo Y, Lee S, Seo MS, Hong IS, Choi SW, Seo KW, Nunez G, Park JH, Kang KS. Human umbilical cord blood mesenchymal stem cells reduce colitis in mice by activating NOD2 signaling to COX2. Gastroenterology. 2013;145(6):1392–403, e1–e8.
16. Nasuno M, Arimura Y, Nagaishi K, Isshiki H, Onodera K, Nakagaki S, Watanabe S, Idogawa M, Yamashita K, Naishiro Y, Adachi Y, Suzuki H, Fujimiya M, Imai K, Shinomura Y. Mesenchymal stem cells cancel azoxymethane-induced tumor initiation. Stem Cells. 2014;32(4):913–925.
17. Lin Y, Lin L, Wang Q, Jin Y, Zhang Y, Cao Y, Zheng C. Transplantation of human umbilical mesenchymal stem cells attenuates dextran sulfate sodium-induced colitis in mice. Clin Exp Pharmacol Physiol. 2015;42(1):76–86.
18. Harizi H, Juzan M, Moreau JF, Gualde N. Prostaglandins inhibit 5-lipoxygenase-activating protein expression and leukotriene B4 production from dendritic cells via an IL-10-dependent mechanism. J Immunol. 2003;170(1):139–146.
19. Voswinkel J, Francois S, Simon JM, Benderitter M, Gorin NC, Mohty M, Fouillard L, Chapel A. Use of mesenchymal stem cells (MSCs) in chronic inflammatory fistulizing and fibrotic diseases: a comprehensive review. Clin Rev Allergy Immunol. 2013;45(2):180–192.
20. Tanaka H, Arimura Y, Yabana T, Goto A, Hosokawa M, Nagaishi K, Yamashita K, Yamamoto H, Sasaki Y, Fujimiya M, Imai K, Shinomura Y. Myogenic lineage differentiated mesenchymal stem cells enhance recovery from dextran sulfate sodium-induced colitis in the rat. Journal of gastroenterology. 2011;46(2):143–152.
21. Rui Y, Xu L, Chen R, Zhang T, Lin S, Hou Y, Liu Y, Meng F, Liu Z, Ni M, Tsang KS, Yang F, Wang C, Chan HC, Jiang X, Li G. Epigenetic memory gained by priming with osteogenic induction medium improves osteogenesis and other properties of mesenchymal stem cells. Sci Rep. 2015;5:11056.
22. Chen R, Lee WY, Zhang XH, Zhang JT, Lin S, Xu LL, Huang B, Yang FY, Liu HL, Wang B, Tsang LL, Willaime-Morawek S, Li G, Chan HC, Jiang X. Epigenetic modification of the CCL5/CCR1/ERK axis enhances glioma targeting in dedifferentiation-reprogrammed BMSCs. Stem Cell Rep. 2017;8(3):743–757.
23. Liu Y, Jiang X, Zhang X, Chen R, Sun T, Fok KL, Dong J, Tsang LL, Yi S, Ruan Y, Guo J, Yu MK, Tian Y, Chung YW, Yang M, Xu W, Chung CM, Li T, Chan HC. Dedifferentiation-reprogrammed mesenchymal stem cells with improved therapeutic potential. Stem Cell. 2011;29(12):2077–2089.
24. Luo S, Fu C, Zhang S, Wang J, Fan X, Luo J, Chen R, Hu X, Qin H, Li C, Ou S, Li Q, Chen S. [Application of SNP-array technology in the genetic analysis of pediatric patients with

growth retardation]. Zhonghua Yi Xue Yi Chuan Xue Za Zhi. 2017;34(3):321–326.
25. Yin F, Sharen G, Yuan F, Peng Y, Chen R, Zhou X, Wei H, Li B, Jing W, Zhao J. TIP30 regulates lipid metabolism in hepatocellular carcinoma by regulating SREBP1 through the AKT/mTOR signaling pathway. Oncogenesis. 2017;6(6):e347.
26. Cooper HS, Murthy SN, Shah RS, Sedergran DJ. Clinicopathologic study of dextran sulfate sodium experimental murine colitis. Lab Investig. 1993;69(2):238–249.
27. Alex P, Zachos NC, Nguyen T, Gonzales L, Chen TE, Conklin LS, Centola M, Li X. Distinct cytokine patterns identified from multiplex profiles of murine DSS and TNBS-induced colitis. Inflamm Bowel Dis. 2009;15(3):341–352.
28. Lu LL, Liu YJ, Yang SG, Zhao QJ, Wang X, Gong W, Han ZB, Xu ZS, Lu YX, Liu D, Chen ZZ, Han ZC. Isolation and characterization of human umbilical cord mesenchymal stem cells with hematopoiesis-supportive function and other potentials. Haematologica. 2006;91(8):1017–1026.
29. Dave M, Jaiswal P, Cominelli F. Mesenchymal stem/stromal cell therapy for inflammatory bowel disease: an updated review with maintenance of remission. Curr Opin Gastroenterol. 2017;33(1):59–68.
30. Forte D, Ciciarello M, Valerii MC, De Fazio L, Cavazza E, Giordano R, Parazzi V, Lazzari L, Laureti S, Rizzello F, Cavo M, Curti A, Lemoli RM, Spisni E, Catani L. Human cord blood-derived platelet lysate enhances the therapeutic activity of adipose-derived mesenchymal stromal cells isolated from Crohn's disease patients in a mouse model of colitis. Stem Cell Res Ther. 2015;6:170.
31. Banerjee A, Bizzaro D, Burra P, Di Liddo R, Pathak S, Arcidiacono D, Cappon A, Bo P, Conconi MT, Crescenzi M, Pinna CM, Parnigotto PP, Alison MR, Sturniolo GC, D'Inca R, Russo FP. Umbilical cord mesenchymal stem cells modulate dextran sulfate sodium induced acute colitis in immunodeficient mice. Stem Cell Res Ther. 2015;6:79.
32. Yu L, Yan J, Sun Z. D-limonene exhibits anti-inflammatory and antioxidant properties in an ulcerative colitis rat model via regulation of iNOS, COX-2, PGE2 and ERK signaling pathways. Mol Med Rep. 2017;15(4):2339–2346.
33. Takahashi S, Yoshimura T, Ohkura T, Fujisawa M, Fushimi S, Ito T, Itakura J, Hiraoka S, Okada H, Yamamoto K, Matsukawa A. A Novel Role of Spred2 in the Colonic Epithelial Cell Homeostasis and Inflammation. Sci Rep. 2016;6:37531.
34. Bouffi C, Bony C, Courties G, Jorgensen C, Noel D. IL-6-dependent PGE2 secretion by mesenchymal stem cells inhibits local inflammation in experimental arthritis. PLoS One. 2010;5(12):e14247.
35. Nemeth K, Leelahavanichkul A, Yuen PS, Mayer B, Parmelee A, Doi K, Robey PG, Leelahavanichkul K, Koller BH, Brown JM, Hu X, Jelinek I, Star RA, Mezey E. Bone marrow stromal cells attenuate sepsis via prostaglandin E(2)-dependent reprogramming of host macrophages to increase their interleukin-10 production. Nat Med. 2009;15(1):42–49.
36. Kota DJ, Prabhakara KS, Toledano-Furman N, Bhattarai D, Chen Q, DiCarlo B, Smith P, Triolo F, Wenzel PL, Cox CS Jr., Olson SD. Prostaglandin E2 indicates therapeutic efficacy of mesenchymal stem cells in experimental traumatic brain injury. Stem Cell. 2017;35(5):1416–1430.
37. Nam YS, Kim N, Im KI, Lim JY, Lee ES, Cho SG. Negative impact of bone-marrow-derived mesenchymal stem cells on dextran sulfate sodium-induced colitis. World J Gastroenterol. 2015;21(7):2030–2039.
38. Abraham C, Cho JH. Inflammatory bowel disease. N Engl J Med. 2009;361(21):2066–2078.
39. Forbes GM. Mesenchymal stromal cell therapy in Crohn's disease. Dig Dis. 2017;35(1–2):115–122.
40. Liang X, Ding Y, Zhang Y, Tse HF, Lian Q. Paracrine mechanisms of mesenchymal stem cell-based therapy: current status and perspectives. Cell Transplant. 2014;23(9):1045–1059.
41. Di Sabatino A, Ciccocioppo R, Luinetti O, Ricevuti L, Morera R, Cifone MG, Solcia E, Corazza GR. Increased enterocyte apoptosis in inflamed areas of Crohn's disease. Dis Colon Rectum. 2003;46(11):1498–1507.
42. Iwamoto M, Koji T, Makiyama K, Kobayashi N, Nakane PK. Apoptosis of crypt epithelial cells in ulcerative colitis. J Pathol. 1996;180(2):152–159.
43. Qiu W, Wu B, Wang X, Buchanan ME, Regueiro MD, Hartman DJ, Schoen RE, Yu J, Zhang L. PUMA-mediated intestinal epithelial apoptosis contributes to ulcerative colitis in humans and mice. J Clin Invest. 2011;121(5):1722–1732.
44. Bouma G, Strober W. The immunological and genetic basis of inflammatory bowel disease. Nature reviews Immunology. 2003;3(7):521–533.
45. ten Hove T, van Montfrans C, Peppelenbosch MP, van Deventer SJ. Infliximab treatment induces apoptosis of lamina propria T-lymphocytes in Crohn's disease. Gut. 2002;50(2):206–211.
46. Tilg H, Moschen A, Kaser A. Mode of function of biological anti-TNF agents in the treatment of inflammatory bowel diseases. Expert Opin Biol Ther. 2007;7(7):1051–1059.